SENSITIVITY OF GLOBAL SIMULATIONS TO THE FORMULATION OF THE EVAPORATION OF CONVECTIVE CONDENSATES

P.R. Rowntree
Meteorological Office
Bracknell, U.K.

Summary: Omission of the evaporation of convective condensates from the Meteorological Office global GCM leads to major changes in the tropical rainfall distribution and in the tropical and middle latitude circulation. These changes are assessed with the aid of experiments with a single column model.

1. INTRODUCTION

The Meteorological Office 11-layer general circulation model (GCM) has recently been used in a series of experiments to assess its sensitivity to the evaporation of convective precipitation. Most GCM convection schemes do not explicitly represent this process although it may be argued that there is an implicit representation in some schemes. The results presented here may thus have general relevance for models as well as providing examples of the effects of changes in a convection scheme on the large-scale circulation.

2. MODEL

The Meteorological Office 11-layer general circulation model is very similar in many respects to the 5-layer model described by Corby et al (1977). Saker (1975) provided a detailed description of the first version of the model, including the changes to the vertical finite differencing scheme needed to maintain the energy conservation properties with unevenly spaced levels. The model is a primitive equation global general circulation model with uneven vertical resolution in σ - coordinates ($\sigma = p/p_* =$ pressure/surface pressure) as specified, for example, by Walker and Rowntree (1977). The horizontal grid in the Cyber 205 version used here is 2° latitude by 3° longitude with multi-point east-west filtering of the tendencies in higher latitudes to maintain computational stability. A leap-frog integration scheme with time smoothing and non-linear horizontal diffusion is employed.

This version of the model uses a boundary-layer scheme based on Method I of Clarke (1970) with interactive soil moisture and snow depth similar to that used in the 5-layer model (Slingo, 1982). Evaporation is limited for soil moistures below 5 cm and run off occurs to limit soil moisture to 15 cm. Large-scale precipitation in the form of rain or snow occurs whenever the relative humidity exceeds 100%. The radiation scheme is based on the 'climatological' one described by Corby et al (1977) though the radiative-convective model discussed in section 4

uses a scheme with explicit calculations of radiative fluxes similar to that described by Slingo (1982). The convection scheme is described in the next section.

3. THE CONVECTION SCHEME

The convective parametrization used in the experiments described here was described in detail by Rowntree (1973) while Lyne and Rowntree (1976) discuss its development using GATE data. It is based on the concept of parcel theory modified by entrainment (Riehl 1954 pp 143 ff, Scorer 1958 pp 155 ff, Ludlam 1963 p 19) with a treatment of detrainment based partly on Ceselski (1972 p 102) and his discussion of the scheme of Arakawa (1969). We imagine an ensemble of buoyant plumes of varying characteristics (temperature, humidity, cross-sectional area) starting at one level and extending upwards to different heights depending on their characteristics. The plumes entrain environmental air over their leading and side surfaces as they push into the environmental air; the less buoyant plumes terminate through lack of buoyancy and detrain at a lower level than more buoyant ones which, perhaps because of their original large cross-section or the more favourable nature of the local environment into which they have risen, have led more protected lives and may even reach the heights accessible to an undilute parcel. Since detrainment is generally assumed to occur with zero buoyancy, the heating of the environment occurs, as in Arakawa's scheme, mainly through the mass descent which compensates the ascent of the buoyant plumes, although moistening by detrainment and re-evaporation of condensed moisture do mitigate the drying and warming effects of this descent.

In more detail, for each model column we work upwards until we find a level at which a parcel starting with a small excess buoyancy relative to the environment will still be buoyant after rising to the next level and entraining some environment air en route. If at this next level it still has an excess buoyancy greater than a certain lower limit (equal to that given to the starting parcel) the convective process is initiated.

At each level the ensemble reaches we calculate whether, after allowing for entrainment between that level and the next the mean ensemble will still be buoyant. If it is not we find what proportion of the less buoyant part of the ensemble needs to be detrained, at a density equal to that of the environment, at the lower level to allow the residue of the ensemble to be buoyant at the next level. (The effects of moisture on density are allowed for both in detrainment and in the buoyancy test). Because the detrainment allows an indefinite extrapolation towards greater buoyancy it is necessary to limit it. A simple restriction is that even the most buoyant plumes should not rise higher than an undilute parcel would. It also seems reasonable to place a lower limit on the mass flux on the assumption that an ensemble of small total cross-section will be

killed by entrainment. Where these restrictions bring the convective process to an end, it is simplest to detrain the residual air with non-zero buoyancy although a scheme could no doubt be worked out in which this was avoided by splitting the detrainment between two layers. The search for further mutually unstable layers is resumed in the layer above that in which this final detrainment occurs.

We have said nothing so far about saturation, condensation or evaporation. The scheme is applicable equally to dry and moist convection, although it is obviously necessary to know which is appropriate at any particular level as certain terms (eg latent heat release) are absent in dry convection and the moisture content of detrained air is defined differently in the two cases.

It may be useful to summarize the basic principles of the scheme and at the same time define quantitatively the version of the scheme used here.

(a) The initial mass flux (M_I) of the ensemble is proportional to the buoyancy E of air taken to a layer from the layer below with an excess (S_θ = 0.2 K) of potential temperature relative to the environment in that lower layer:

$$M_I = (2\Delta t)\ (3.33 \times 10^{-7} s^{-1} K^{-1})\ (E/\Delta\sigma)$$

where Δt is the timestep

$$E = \theta^p_{vj} - \theta^e_{vj} - b$$

Here θ^p_{vj} (θ^e_{vj}) is the parcel (environment) virtual potential temperature in layer j and b (equal to 0.2 K) is a minimum excess buoyancy which the ensemble always retains relative to the environmental air. The constant in the expression for M_I has been chosen on the basis of experience with the model so as to maintain continuous convection without an excessively unstable lapse rate. For reasons of computational stability, M_I is not allowed to exceed the thickness of the shallowest model layer. Additionally if M_I is calculated to be less than a minimum value

$$M_{min} = (2\Delta t)\ (3.33 \times 10^{-7} s^{-1})$$

convection is not initiated.

(b) Entrainment of environmental air into the ensemble over a layer of thickness $\Delta\sigma$ at level σ is a prescribed fraction

$$\epsilon = 3\sigma\Delta\sigma$$

of the mass flux M_k. In the absence of detrainment this will double the mass flux of an ensemble initiated in the lowest layer by about 600 mb. The formulation was based loosely on the review of entrainment theory by Lopez (1972) and is given some support by estimates by Byers and Braham (1948) based on balloon convergence observations and aircraft observations.

(c) Detrainment at zero buoyancy relative to the environment occurs only when necessary to maintain the minimum excess buoyancy (b) except that convection terminates with detrainment at positive relative buoyancy when normal detrainment would either (1) reduce mass flux below M_{min}

or (2) increase the buoyancy of the ensemble above that of an undilute parcel.

(d) The environment is modified by net heat and moisture convergence due to:

(1) compensating subsidence

(2) entrainment

(3) detrainment

(4) evaporation of condensates

and (5) melting of snow

after adjusting temperature increments to ensure conservation of energy ($C_p T + Lq$) (where C_p is specific heat of air, L is latent heat coefficient and T and q are temperature and specific humidity).

(e) The evaporation in layer k of convective condensates formed when the ensemble rises from layer k to layer (k-1) in g $cm^{-2}/2\Delta t$ is

$$C_{EV} M_{k-1} (q_s(T_k^e)-q_k^e) \quad (10p_*\Delta\sigma/g)$$

where C_{EV} is an arbitrary constant, $q_s(T_k^e)$ the saturation specific humidity of air in layer k, q_k the specific humidity in layer k, and g the acceleration due to gravity.

This is intended mainly to represent the evaporation of cloud water and ice and precipitation cannot be evaporated after falling below layer k. (In a version of the scheme developed since the experiments described here, this restriction has been relaxed to allow evaporation of falling precipitation but only below cloud base with evaporation of cloud water, which can now be carried upwards in the ensemble, occurring through a prescribed detrainment of cloud air.)

It is possible to estimate the fraction of the condensate which will be evaporated with the above scheme. The precipitation generated in taking the ensemble from layer k to layer (k-1) is at most

$$M_{k-1}\ (q_s(T^p_k)-q_s(T^p_{k-1}))\ (10p*/g)$$

so that

$$\frac{\text{Evaporation}}{\text{Precipitation}} \gtrsim \frac{C_{EV}(1-RH_k)q^e_{s_k}\,\Delta\sigma_k}{q_s(T^p_k)-q_s(T^p_{k-1})}$$

$$\approx \frac{C_{EV}\ (1-RH_k)}{(\partial q_s/\partial\sigma)_{k-\frac{1}{2}}/q^e_{s\,k}}$$

Here RH is relative humidity. Typically $(\partial q_s/\partial\sigma)_{k-\frac{1}{2}}/q_{sk}$ is 2.5 below 700 mb increasing upwards to about 5 at 500 mb, so that the condition for total evaporation, neglecting the drying effects of entrainment, is,

with $C_{EV} = 9$ RH $\leq$ 72% below 700 mb

and RH $\leq$ 44% near 500 mb

4. EFFECTS OF CONVECTION ON THE ENVIRONMENT IN A RADIATIVE-CONVECTIVE MODEL

It is appropriate here to consider in more detail the effects of the convection on the environment. These are proportional to the mass flux M_k, and may be separated into three components, associated with subsidence compensating the ascent in the buoyant plumes, the detrainment from the buoyant plumes and the evaporation of the condensate either as cloud liquid water or precipitation.

The environment is brought towards a lapse rate similar to that followed by the convective ensemble which is more or less close to the moist adiabatic depending on how dry the entrained air is. If the environment is more stable than the ensemble ascent, the ensemble loses buoyancy and detrains so reducing δT and δq at higher levels and allowing radiative cooling to destabilise the environment in the absence of subsidence. The complete derivatives of T and q with respect to time may be written in brief as shown here

$$\delta T = \delta T(\underset{-}{SUB}) + \delta T(\underset{+}{DET}) + \delta T(\underset{-}{EV}) + \delta T(\underset{+}{ADV}) + \delta T(\underset{+}{BL}) + \delta T(\underset{+}{LSR}) + \delta T(\underset{-}{RAD})$$

$$\delta q = \delta q(\underset{+}{SUB}) + \delta q(\underset{+}{DET}) + \delta q(\underset{+}{EV}) + \delta q(\underset{+}{ADV}) + \delta q(\underset{+}{BL}) + \delta q(\underset{-}{LSR})$$

SUB-SIDENCE; DETRAIN-MENT; EVAPOR-ATION; ADVEC-TION; BOUNDARY LAYER; LARGE SCALE RAIN; RADIA-TION

The signs below each term are appropriate for the conditions of ascent and upward surface moisture flux in which convection is important. Some simplification is

possible. In this model 'large scale rain' associated with super saturation of the whole grid box is usually small at least in the tropics. The effects on temperature of detrainment at neutral buoyancy are small. The turbulent heat flux is also often small. Above the boundary layer, then, subsidence is opposed by all the other significant terms in both the T and the q equation.

Here I particularly wish to discuss the effects of the evaporation of convective precipitation. Let us first consider the situation with no advection - the radiative-convective model (RCM) context. In the T equation, subsidence heating balances radiative cooling. Note that if the final θ profile is essentially determined by q through convection, this means that the mass fluxes M are determined by q and the radiative cooling; also because evaporation opposes subsidence, M must increase as C_{EV} increases for a given q profile.

In the q equation, without evaporation, subsidence drying can only be balanced by detrainment moistening. This implies that where no detrainment occurs, the vertical gradient of q must vanish. This result can be seen in the RCM with $C_{EV} = 0$ at Day 20 of an experiment with land surface boundary conditions (Fig. 1). Figure 2 shows the effect of zeroing C_{EV} on the RCM over sea (i.e. with fixed surface temperatures). The vertical roughness is a consequence of the mechanism just discussed. The general drying above the boundary layer is to be expected from the removal of the evaporative moisture source. The greater drying over land is a transient feature associated with more intense convection though during the subsequent warming relative humidities are reduced more over the land. The boundary layer moistening is a consequence of the decrease in mass flux caused by the lack of evaporative cooling to oppose subsidence heating and of the major moistening role of surface fluxes previously opposed more strongly by subsidence drying. This feature is important because it reduces surface turbulent fluxes over the fixed sea surface temperatures but not over the more responsive land surface.

The same happens with temperatures (Figure 3), the warming over the land after only 1 day being nearly 1 K more than over the sea through much of the troposphere. The drying of the air leads to a steeper lapse rate and so a marked upper tropospheric cooling by Days 16-20. The lapse rate over land is less because of the temperature dependence of the moist adiabatic lapse rate - a 2 K surface warming will warm the upper troposphere about 5 K for a moist adiabatic lapse rate. Although the land is still warmer at this time a decline has started due to the effects of the drying on the interactive radiation scheme used in this model; with less water vapour the radiation leaving the atmosphere comes from lower, warmer levels. By Day 100, the cooling is between 3 and 12 K, by Day 500 from 11 to 28 K. Though not very relevant to land in an atmospheric GCM because of the moderating

influence of fixed ocean temperatures, it would be very relevant to a climate model with the ocean allowed to vary.

5. EFFECTS ON GCM SIMULATIONS OF ELIMINATING EVAPORATION OF CONVECTIVE RAINFALL

(a) First 10 days

The one-dimensional (RCM) results suggested that a reduction in C_{EV} would initially dry the atmosphere except in the lowest two layers, with a warming which is greater over land than sea and which decays after the first few days. The Day 1-10 mean differences at σ = .718 (Fig. 4) clearly show the expected drying with much of the (shaded) negative area having decreases of 2 to 4 x 10^{-3}. There is little drying north of 30°N over land where there is little convective precipitation. As in the RCM, the lowest two layers are moister everywhere that one of the models has precipitation in the area shown in Fig. 5 except near 45°N 180°.

The temperature differences in the upper troposphere are also as expected with warming of about 1 K over land and cooling of up to 2 K at σ = .317 over the sea (Fig. 6). A more general warming is evident at σ = .718 (Fig. 7) but again, as expected, with the maximum over land; however some of the differences over India may be complicated by differences in the monsoon onset found in experiments by Kershaw (1984). The same may apply to the differences at σ = .987 (Fig. 8) which again show a greater warming over land than sea, apart from the warming over the tropical northwest Pacific.

It is instructive at this point to consider Kershaw's results for Day 4 of forecasts from FGGE analyses for 12 GMT 11 June 1979 with C_{EV} = 0 and 9. The sea level pressure maps (Fig. 9) show that the forecast with C_{EV} = 9 has a much weaker geostrophic westerly over India than that with C_{EV} = 0 with the latter having lower pressure at 25°-30°N by about 5 mb and as high pressure south of the equator. This is what would be expected hydrostatically from the temperature differences which are similar to those shown in Figures 6-8. The contrast is even more striking in the 850 mb winds (Fig. 10). With C_{EV} = 9 there has been little advance in the monsoon westerly maximum from the initial time whilst with C_{EV} = 0 speeds exceed 8 ms^{-1} over much of the Bay of Bengal and India compared with less than 4 ms^{-1} with C_{EV} = 0. Rainfall (not shown) is also very different with large areas of over 5 mm/day over India with C_{EV} = 0 but not with C_{EV} = 9 and quite different distributions over the ocean. A shift of convective activity from ocean to land is very clear at this stage; averaged over Days 1-10 of the GCM experiment, rainfall over land (mostly convective) is increased by 3.3 mm/day at 0°-20°N with little change over the ocean. This difference becomes much less pronounced later.

The Day 1-10 rainfall difference distribution (Fig. 11) is to a substantial extent consistent with a general transfer from ocean to land but there are important departures again notably over the west Pacific at 0°-20°N. Wind difference maps for 850 mb show that the Indian Ocean monsoon westerlies extend much further east with $C_{EV} = 0$ (as suggested by Fig. 10), converging more strongly in the west Pacific.

(b) Days 21-50

The differences at Days 21-50 are sufficiently similar to those at Days 1-10 for the previous discussion to be generally relevant. At $\sigma = .718$ the q differences (not shown) are now 2 to 5 x 10^{-3} while at $\sigma = .987$ there is also not much difference apart from large decreases over northwest India and Pakistan where a drying of the surface has led to a very different regime with much higher temperatures at low levels as shown in Fig. 12 for $\sigma = .987$. Elsewhere over land warming is less widespread than at Days 1-10 while over the sea there is little change; this is what one would expect from the RCM's results, with the initial warming decaying. Note the persistence of warming over the west Pacific; this region depends on low-level convergence more than surface evaporation as its moisture source for precipitation in the model. It is typically too warm in the model compared with reality with a temperature profile close to the moist adiabatic in experiments with $C_{EV} = 9$. This is clearly less so with $C_{EV} = 0$ as shown by the temperature differences at $\sigma = .718$ (Fig. 13), due to the drier character of the middle troposphere. At this level the run with $C_{EV} = 0$ is still warmer over eastern and central Asia but not over all continents.

This is also true at $\sigma = .317$ (Fig. 14) where temperatures generally are reduced by 3 to 6 K in the tropics. The warming over central and eastern Asia together with the large cooling over the central North Pacific evident at $\sigma = .718$ and .317 appears to be associated with major planetary wave changes in middle latitudes, also evident in the sea level pressure differences.

Over the northern hemisphere generally (Fig. 15) pressure is lower over land and higher over the ocean though there are notable exceptions over the western tropical Pacific and eastern North Atlantic. The phase of the differences in the tropics and the summer subtropics and middle latitudes tends to reverse with height as shown by the wind differences at 200 and 850 mb, indicating a baroclinic structure. There are more intense features at 30°N to 30°S than in higher latitudes at Days 1-10 while wind differences are similar in magnitude at Days 21-50 perhaps indicating that perturbations originate in the tropics and propagate to higher latitudes. Though the North Pacific high is already well developed at Days 1-10 it is barotropic in structure at that time suggesting it is initially remotely forced, unlike features both to the south and west near 120°-135°E.

The most marked change between the Day 21-50 pressure patterns (Fig. 16) is in the North Pacific high. Near the North American coast with $C_{EV} = 9$, it is transferred to mid-Pacific and intensified; the falls off China lead to much stronger southerlies over the west Pacific. Over the Atlantic the ridge to Europe from the Azores high moves north. Very similar differences to these were obtained in the tropics and northern hemisphere in an earlier run with minor differences in the evaporation over land and also from a subsequent integration with interactive radiation except that the changes near western Europe and over west Africa were much weaker.

The precipitation differences at Days 21-50 (Fig. 17) are in many respects similar to those at Days 1-10 (Fig. 11). The similarities over the Indian Ocean south of India are particularly striking. The increases in rainfall over land are less widespread than at Days 1-10, with marked decreases over parts of the Indian sub-continent, particularly the northeast.

References

Arakawa, A. 1969 Parametrization of cumulus convection. Proceedings of WMO/IUGG Symposium on Numerical Weather Prediction, Tokyo. (Japan Met. Agency Tech. Report 67), pp. IV - 8-1 to IV - 8-6.

Byers, H.R. and R.R. Braham, Jr. 1948 Thunderstorm structure and circulation. J.Met., 5, 71-86.

Ceselski, B.F. 1972 A comparison of cumulus parametrization techniques in numerical integrations of an easterly wave. Report 72-1 (Part 4), Dept. Met. Florida State University, Tallahassee.

Clarke, R.H. 1970 Recommended methods for the treatment of the boundary layer in numerical models. Australian Met. Mag., 18, 51-57.

Corby, G.A., A. Gilchrist and P.R. Rowntree 1977 The U.K. Meteorological Office 5-layer general circulation model. Methods in Computational Physics, 17, 67-110.

Kershaw, R. 1984 The sensitivity of forecasts of the onset of the southwest monsoon to changes in model formulation. Met O 20 Tech. Note II/216, Meteorological Office, Bracknell.

Lopez, R.E. 1972 A parametric model of cumulus convection. Atmospheric Science Paper No. 188, Colorado State University, Fort Collins.

Ludlam, F.H. 1963 Severe local storms - a review. Meteorological Monographs, 5, 1-30, Amer. Met. Soc.

Lyne, W.H. and P.R. Rowntree 1976 Development of a convective parametrization using GATE data. Met O 20 Tech. Note II/70, Meteorological Office, Bracknell

Riehl, H. 1954 Tropical meteorology. McGraw Hill, New York.

Rowntree, P.R. 1973 Proposed convection scheme for the 11-layer tropical model. Unpublished typescript Met O 20, Meteorological Office, Bracknell.

Saker, N.J. 1975 An 11-layer general circulation model, Met O 20 Tech. Note II/30, Meteorological Office, Bracknell.

Scorer, R.S. 1958 Natural Aerodynamics. Pergamon Press, London

Slingo, J.M. 1982 A study of the earth's radiation budget using a general circulation model. Quart. J.R. Met. Soc., 108, 379-405.

Walker, J. and P.R. Rowntree 1977 The effect of soil moisture on circulation and rainfall in a tropical model. Ibid, 103, 29-46.

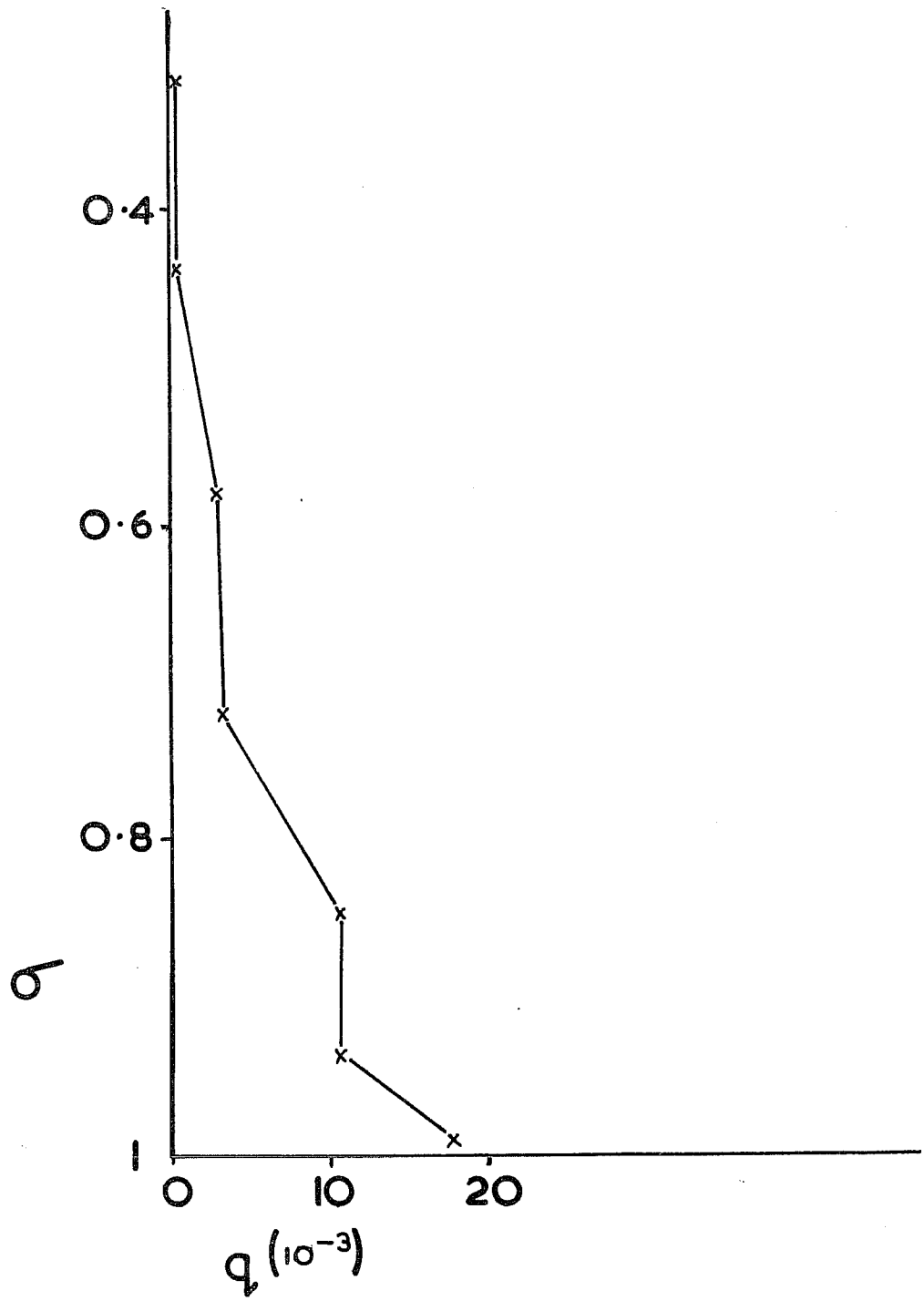

Fig. 1 Specific humidity at Day 20 of RCM experiment for land points with C_{EV}=0.

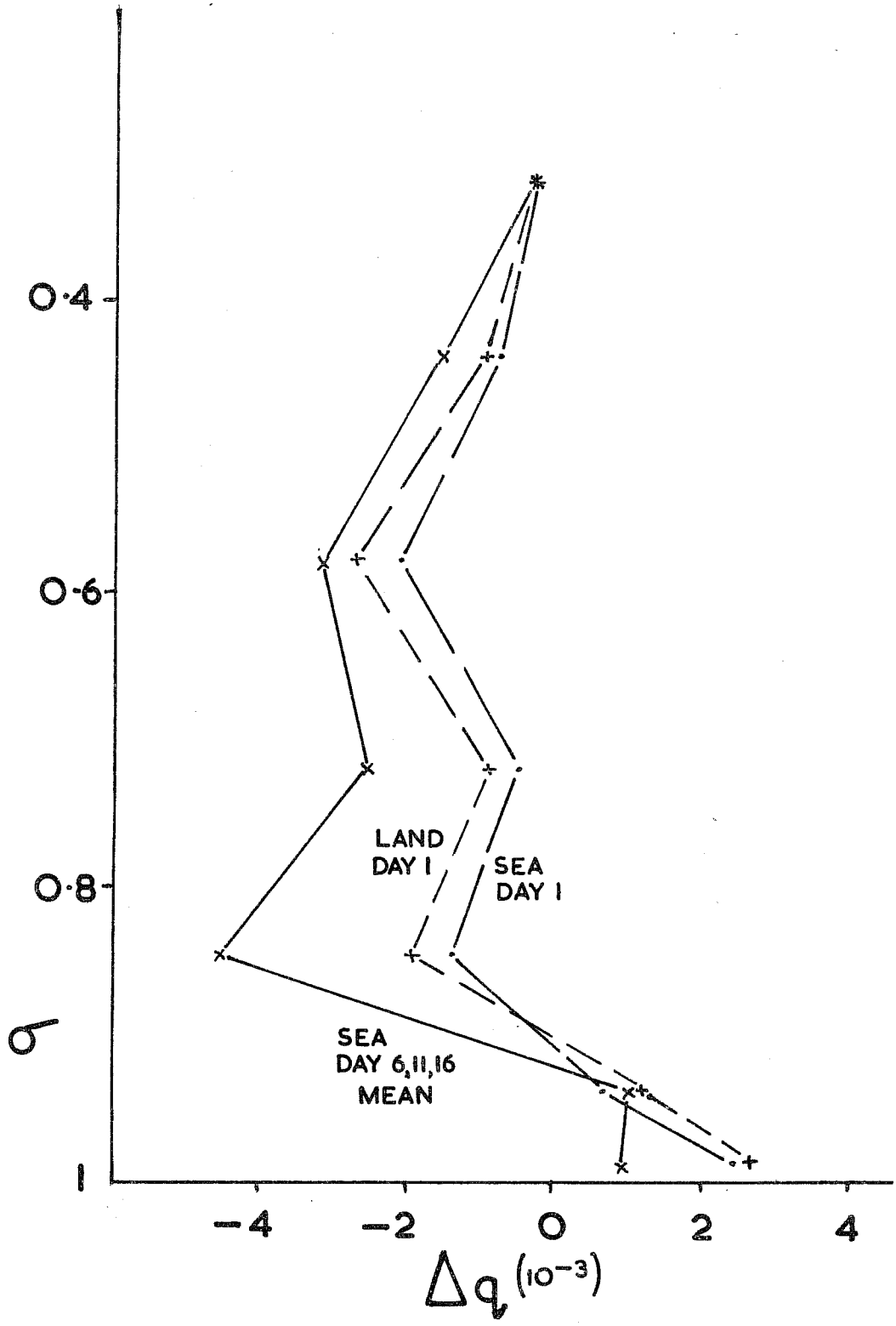

Fig. 2 Effect on specific humidity in RCM experiments of changing C_{EV} from 9 to 0.

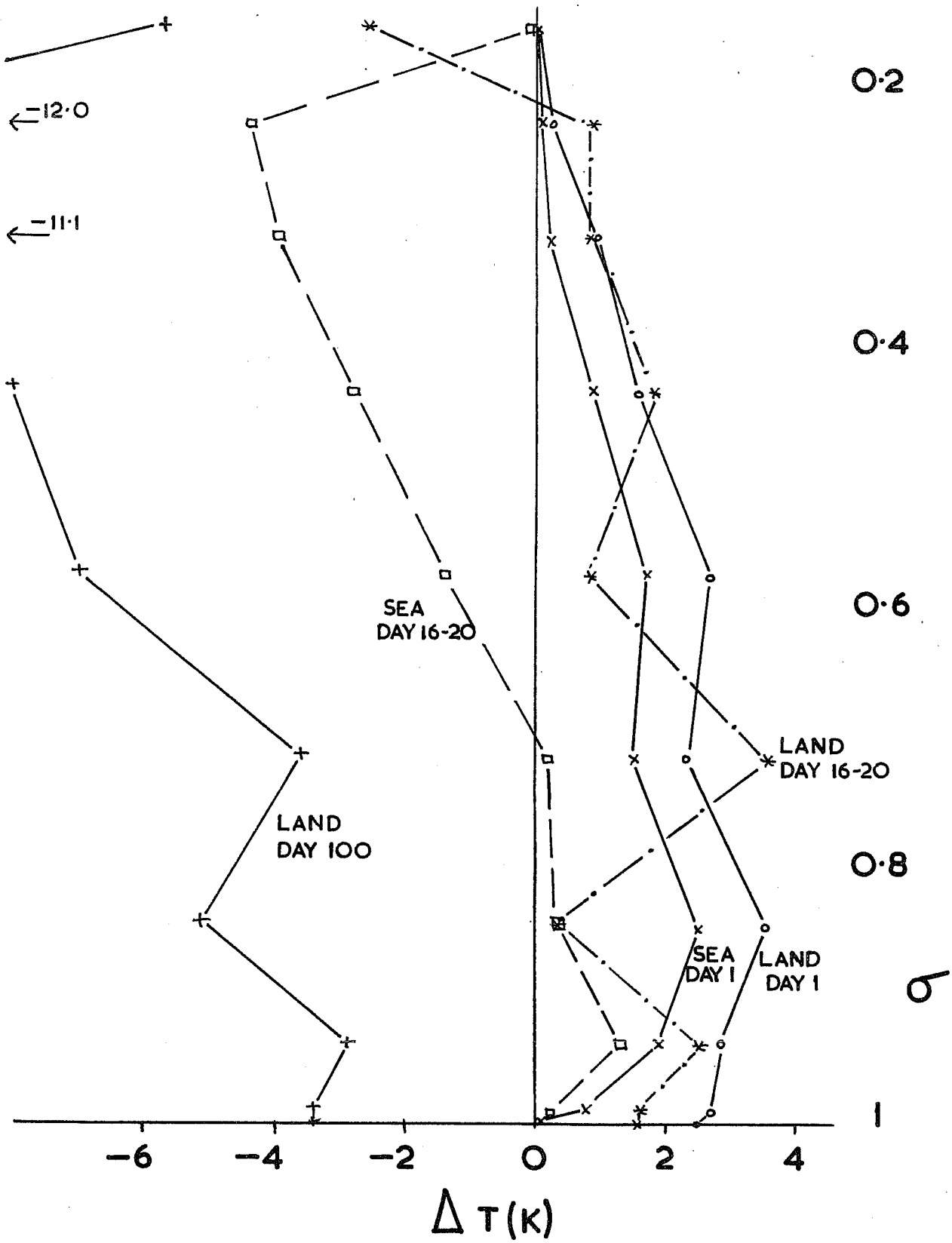

Fig. 3 Effect on temperature in RCM experiments of changing C_{EV} from 9 to 0.

DCA00110 - DCAB0110
SPECIFIC HUMIDITY
AVERAGE FROM 0Z ON 10/6/79 DAY 1 TO 0Z ON 10/6/79 DAY 10
LEVEL: SIGMA=0.718 EXPERIMENT NO.: 1040

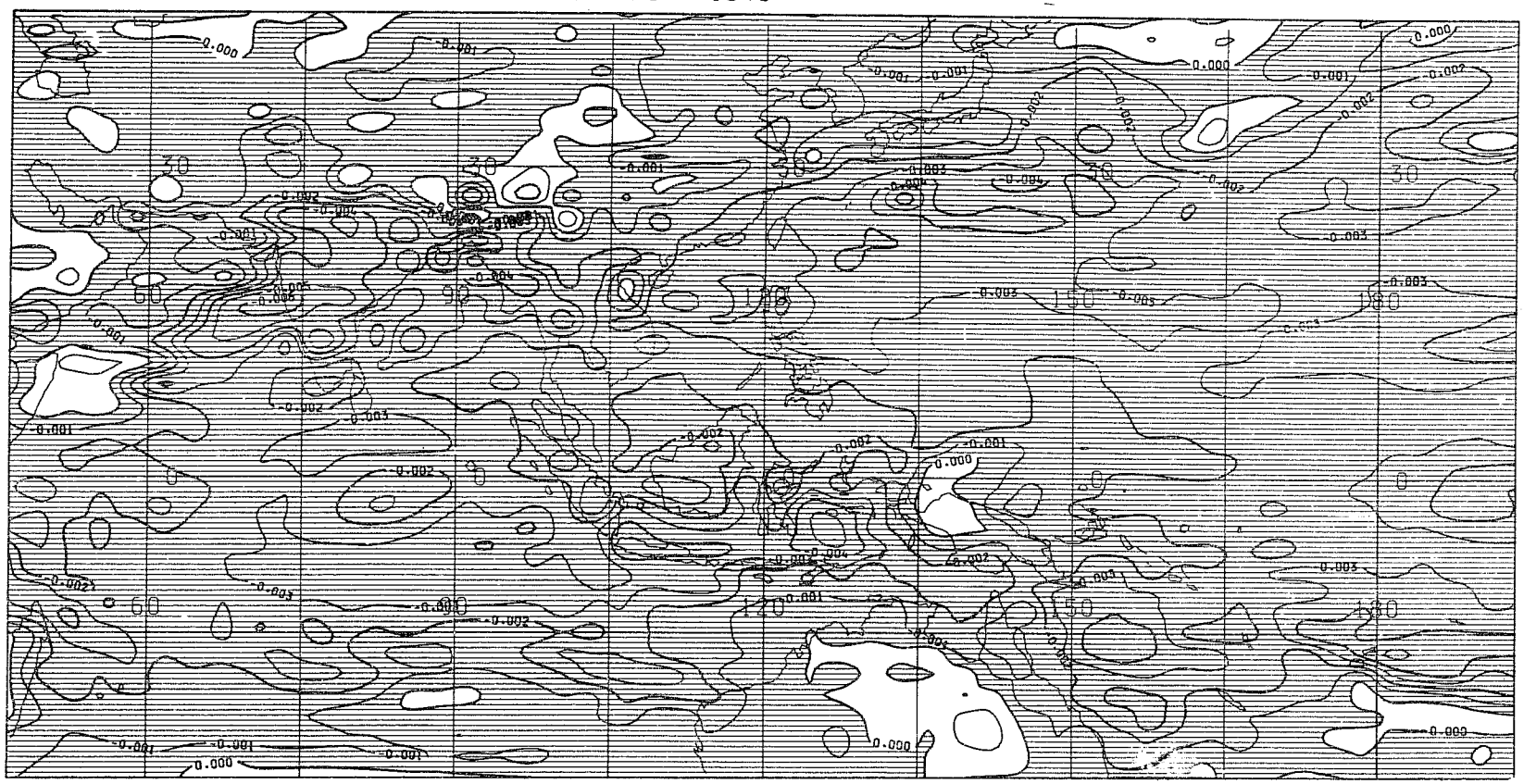

Figure 4 Effect of changing C_{EV} from 9 to 0 on specific humidity at σ =0.718 averaged for Days 1 - 10
Contour interval 10^{-3}; decreases shaded.

DCA00110 - DCAB0110
SPECIFIC HUMIDITY
AVERAGE FROM 0Z ON 10/6/79 DAY 1 TO 0Z ON 10/6/79 DAY 10
LEVEL: SIGMA=0.987 EXPERIMENT NO.: 1040

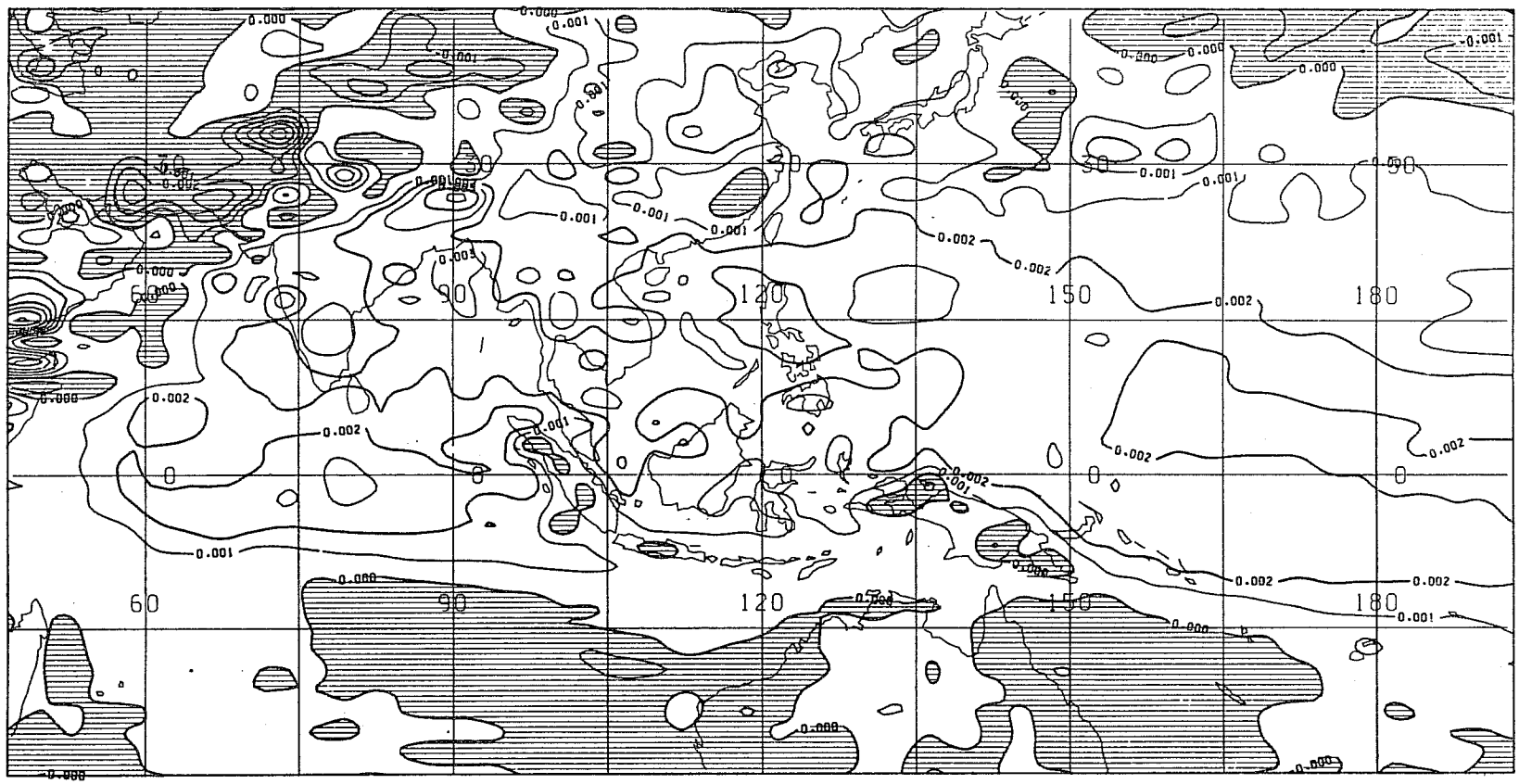

Figure 5 As figure 4 for σ =0.987

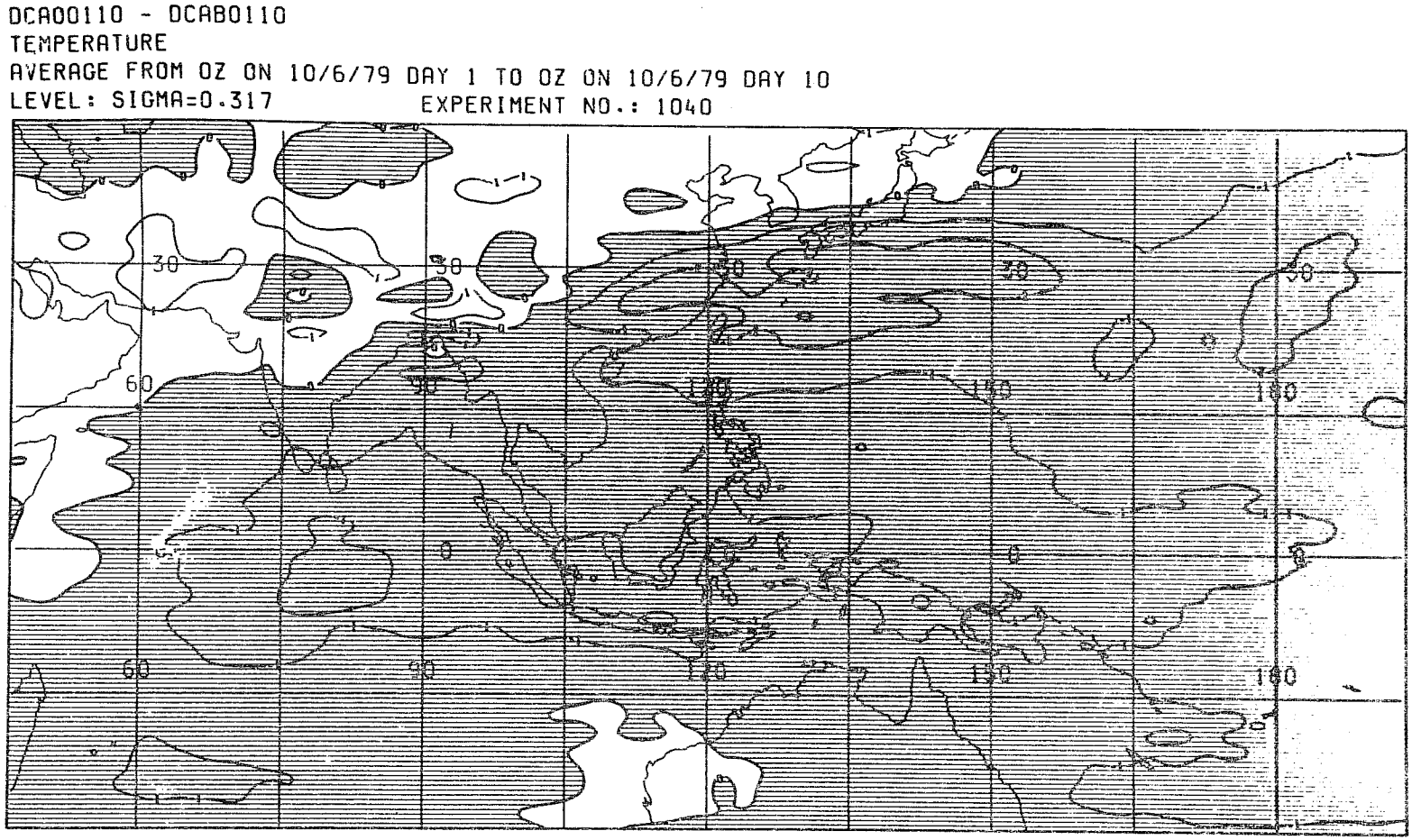

Figure 6 Effect of changing C_{EV} from 9 to 0 on temperature at σ=0.317 averaged for Days 1 - 10
Contour interval 1K; decreases shaded.

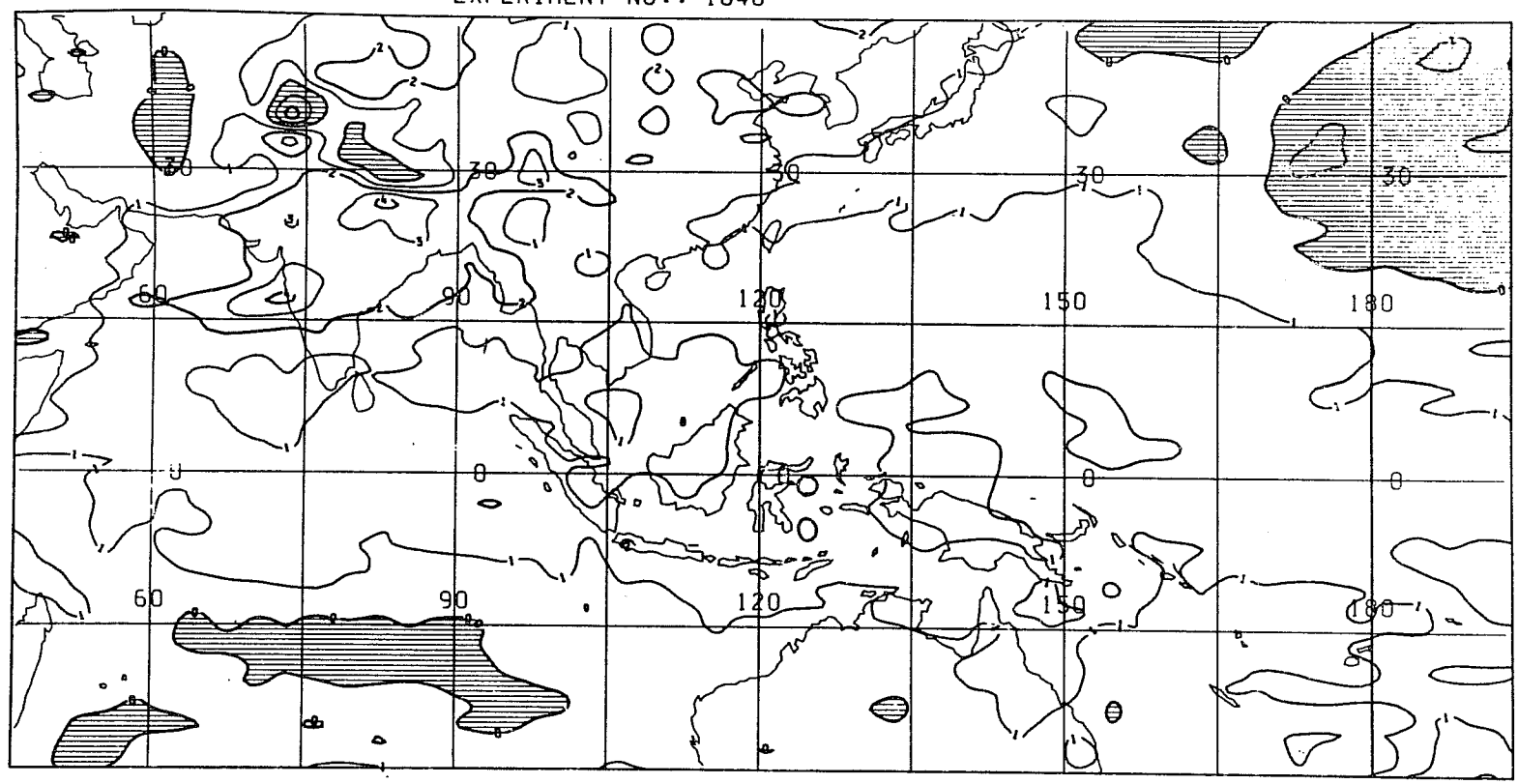

Figure 7 As Figure 6 for σ=0.718

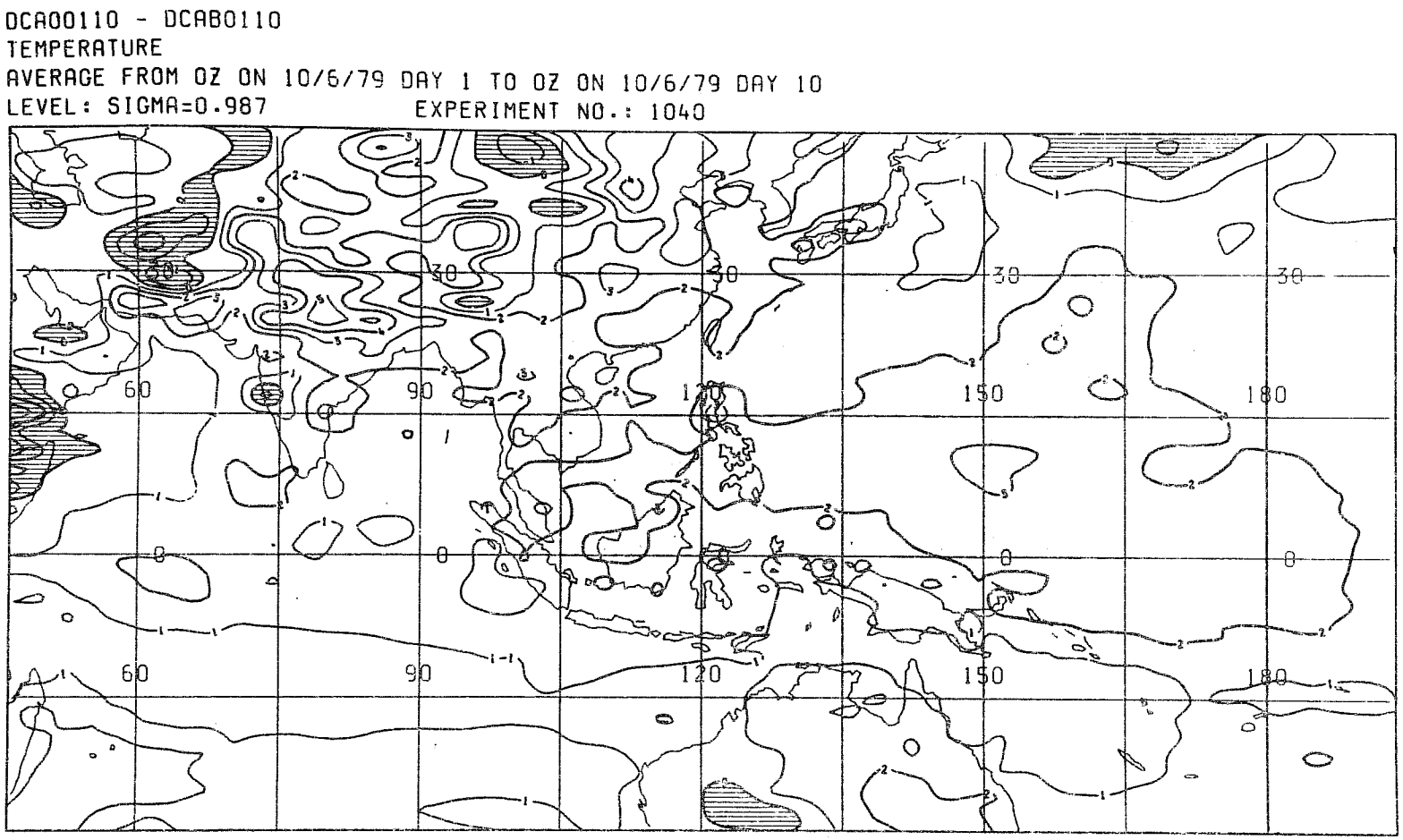

Figure 8 As Figure 6 for σ=0.987

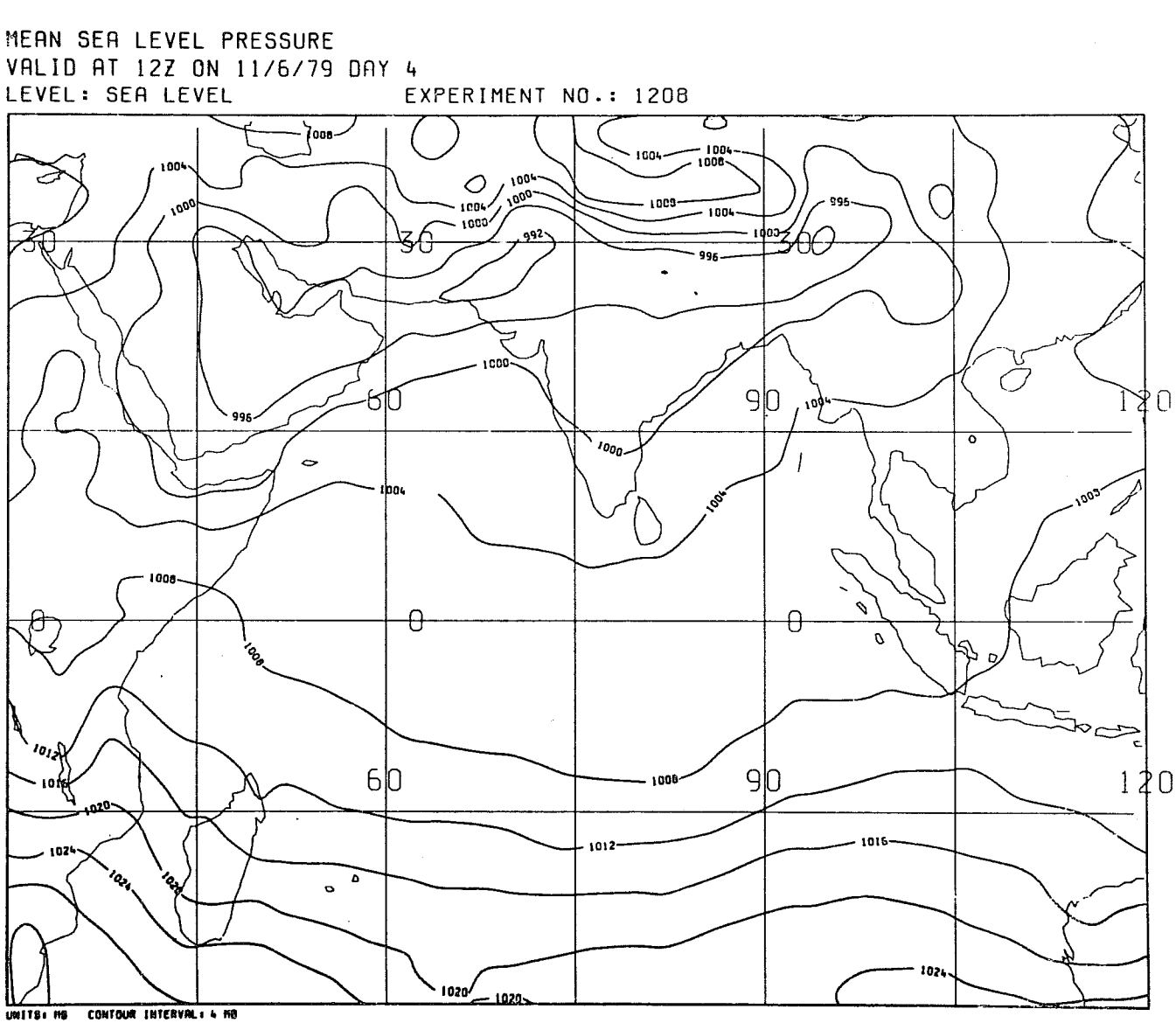

Figure 9(a) Sea level pressure at Day 4 of the experiment by Kershaw (1984) with $C_{EV} = 0$

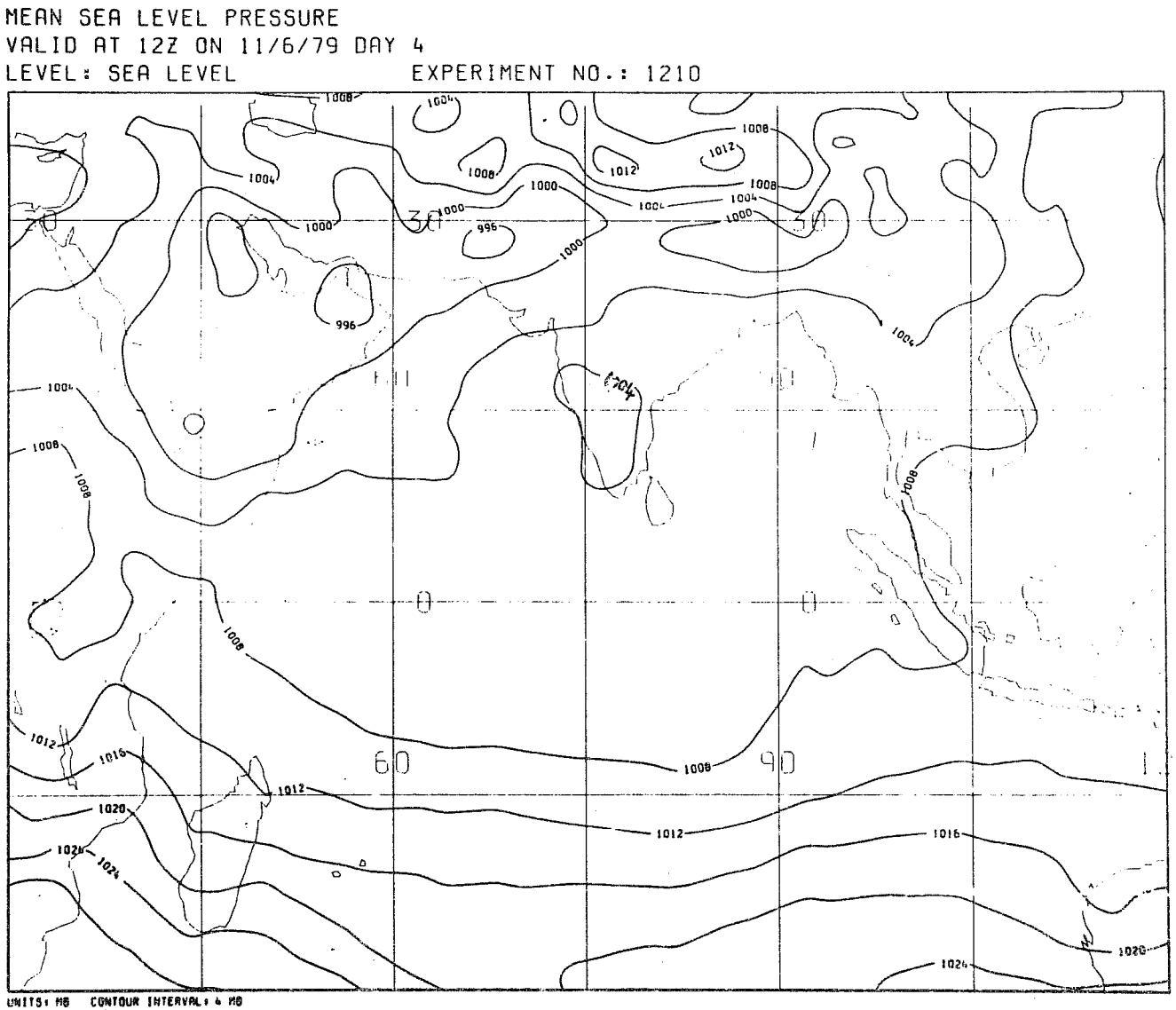

Figure 9(b) As Figure 9(a) with C_{EV} =9

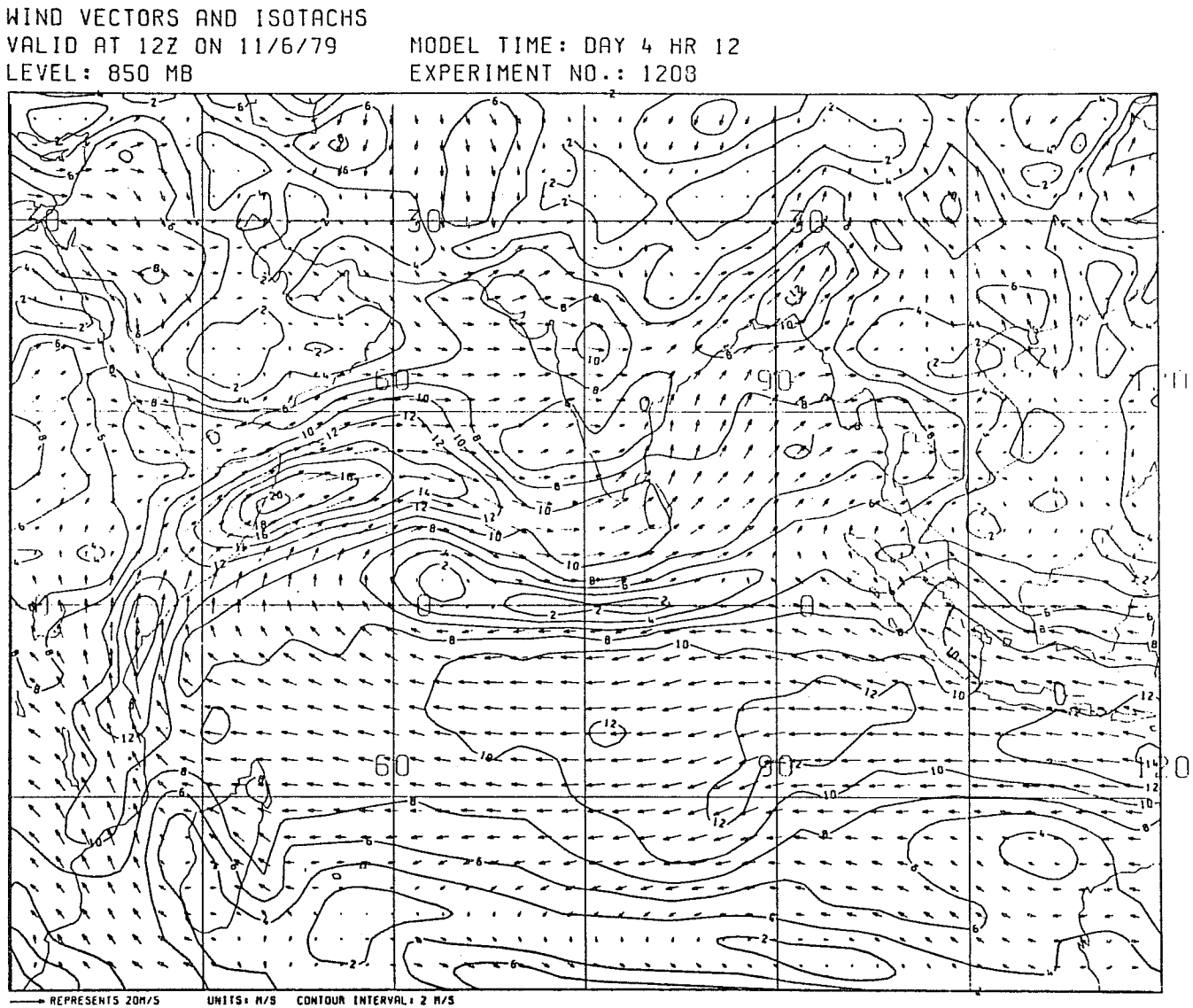

Figure 10(a) As Figure 9(a) for winds at 850mb.

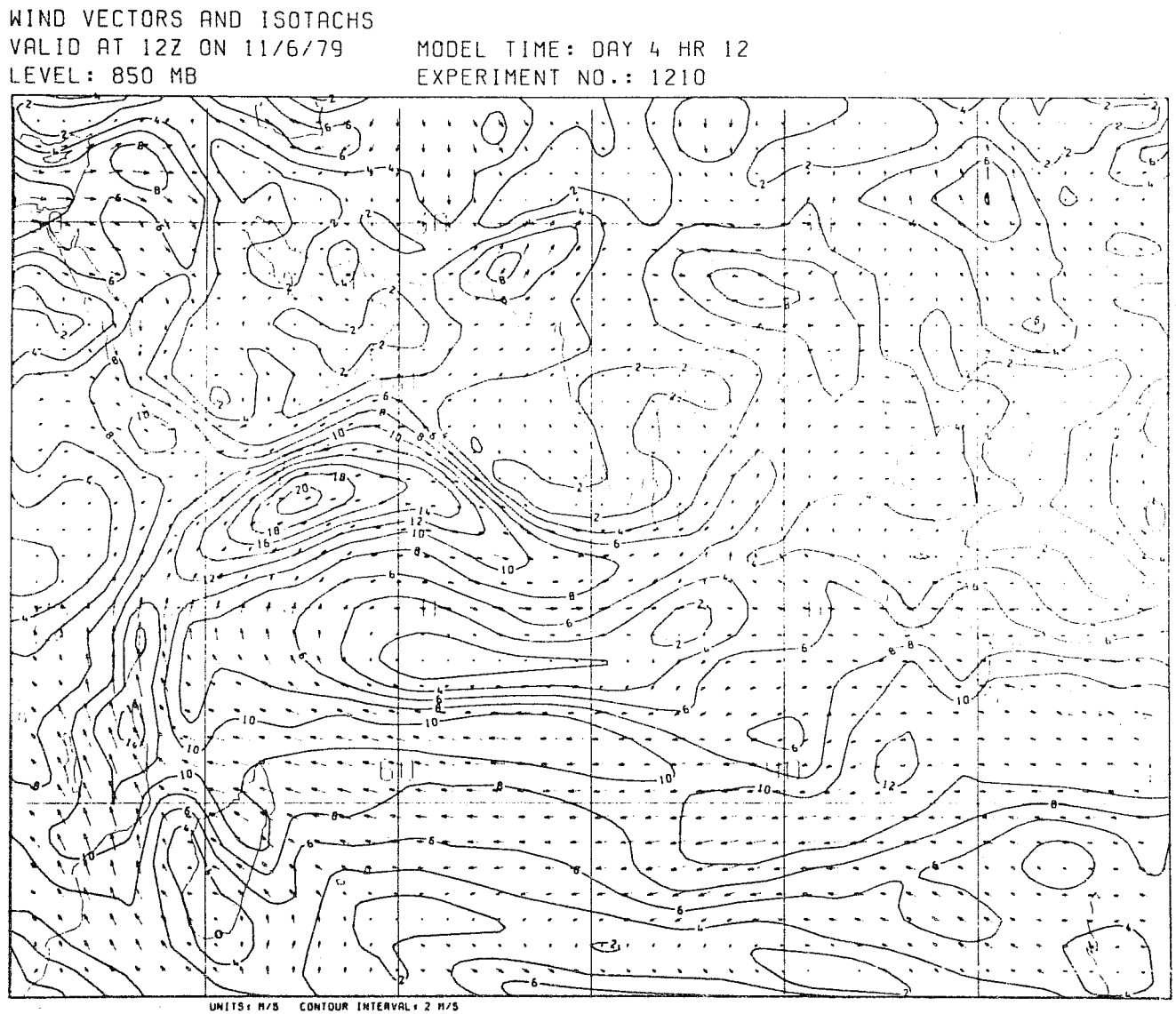

Figure 10(b) As Figure 10(a) with C_{EV} = 9

PRECIPITATION DCA00110 - DCAB0110
FIELD= 94
AVERAGE FROM 0Z ON 10/6/79 DAY 1 TO 0Z ON 10/6/79 DAY 10
LEVEL: SURFACE EXPERIMENT NO.: 1040

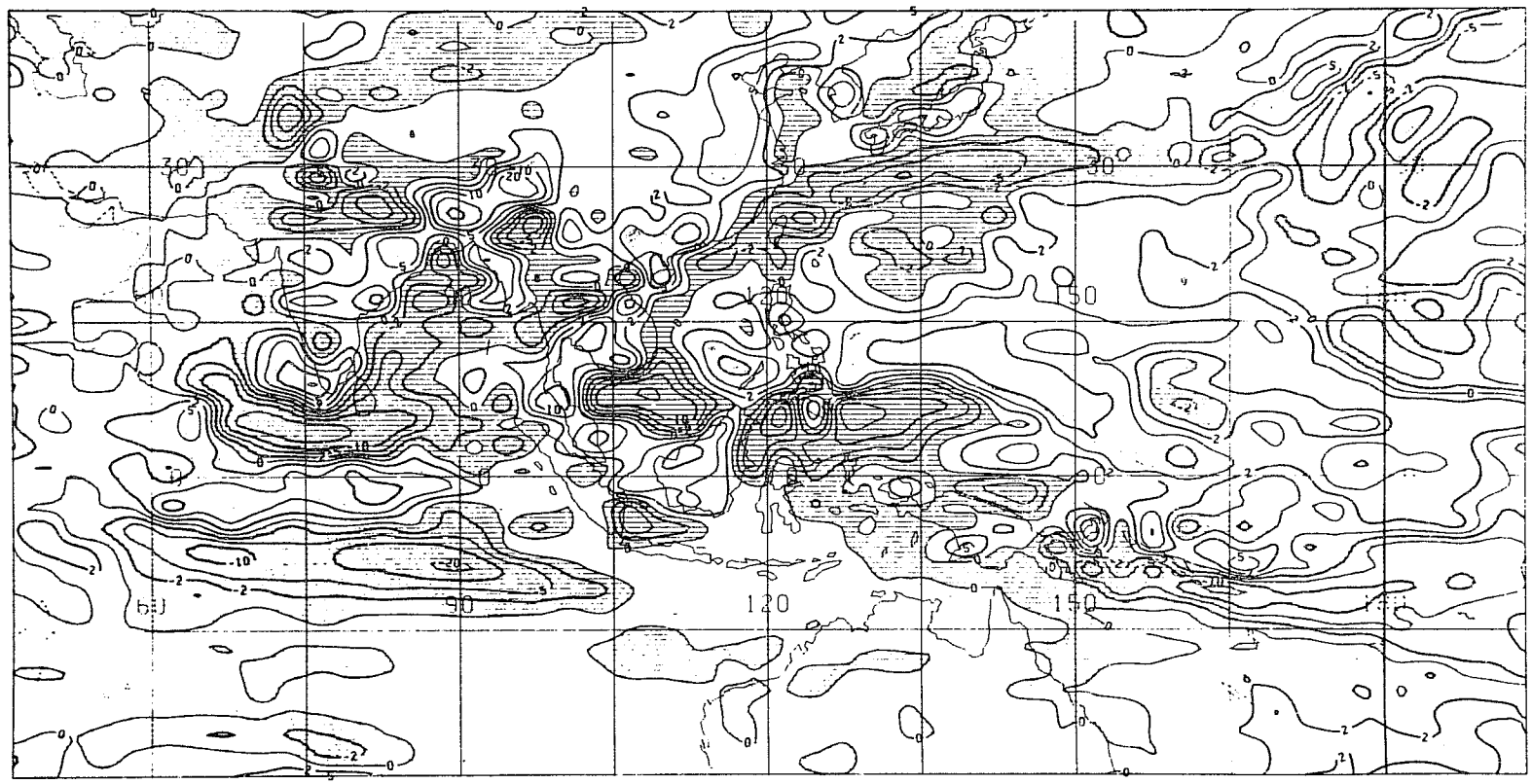

Figure 11 Effect of changing C_{EV} from 9 to 0 on precipitation averaged for Days 1 - 10
Contours at 0, $\pm$ 2,5,10,20,30 mm/day; decreases shaded.

DCA02150 - DCAB2150
TEMPERATURE
AVERAGE FROM 0Z ON 10/6/79 DAY 21 TO 0Z ON 10/6/79 DAY 50
LEVEL: SIGMA=0.987 EXPERIMENT NO.: 1040

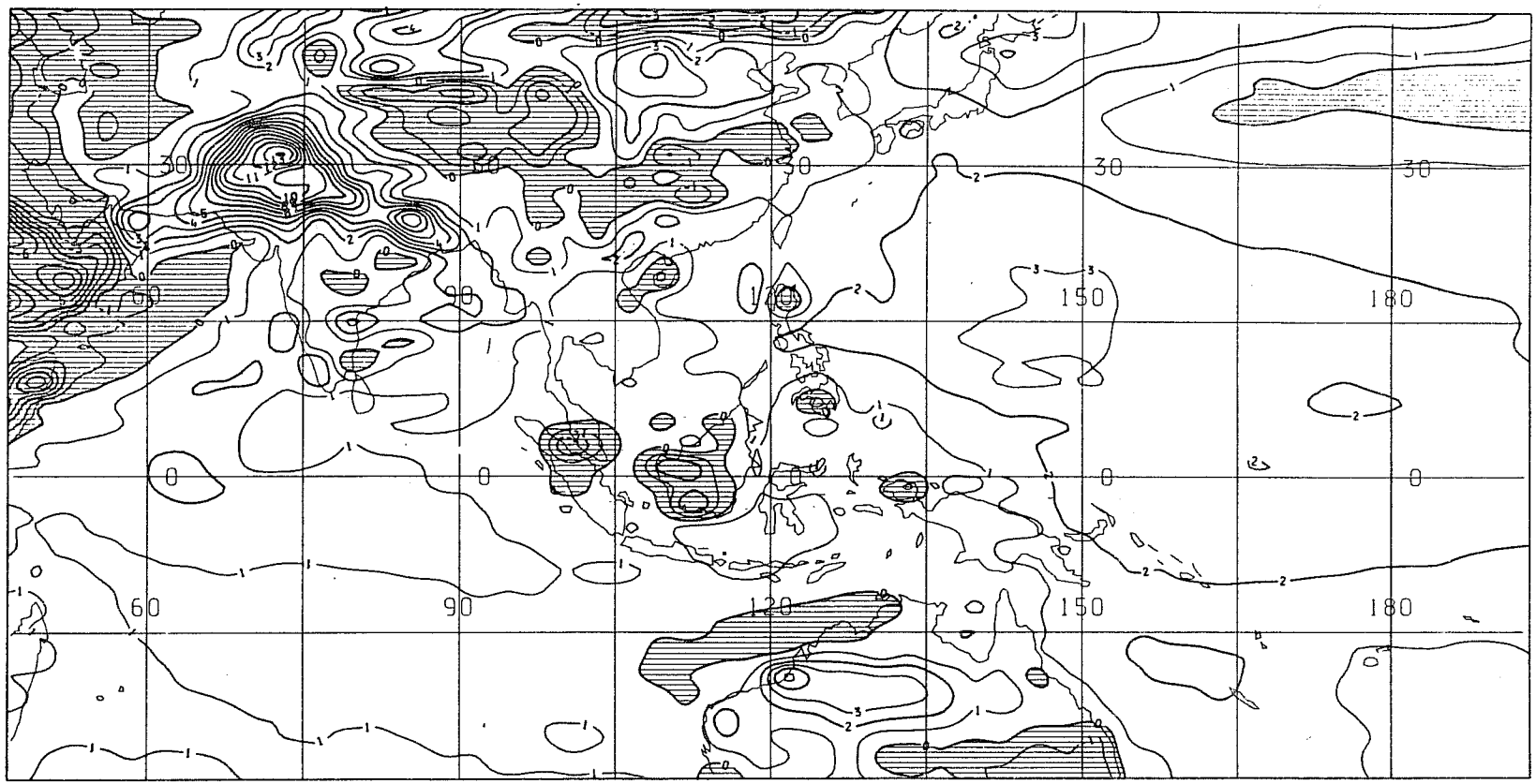

Figure 12 Effect of changing C_{EV} from 9 to 0 on temperature at σ = 0.987 averaged for Days 21 - 50
Contour interval 1K; decreases shaded.

DCA02150 - DCAB2150
TEMPERATURE
AVERAGE FROM 0Z ON 10/6/79 DAY 21 TO 0Z ON 10/6/79 DAY 50
LEVEL: SIGMA=0.718 EXPERIMENT NO.: 1040

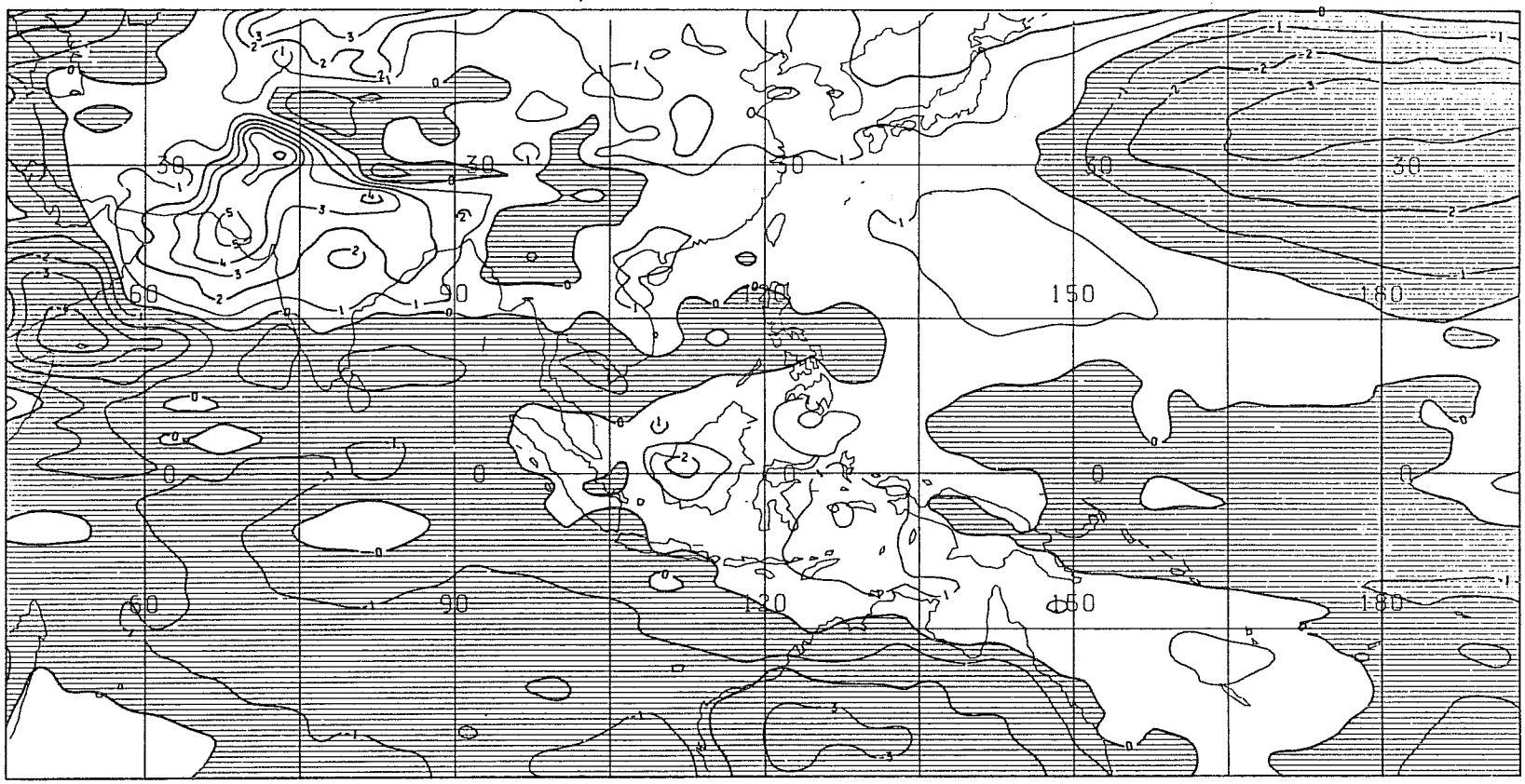

Figure 13 As Figure 12 for σ = 0.718

DCA02150 - DCAB2150
TEMPERATURE
AVERAGE FROM 0Z ON 10/6/79 DAY 21 TO 0Z ON 10/6/79 DAY 50
LEVEL: SIGMA=0.317 EXPERIMENT NO.: 1040

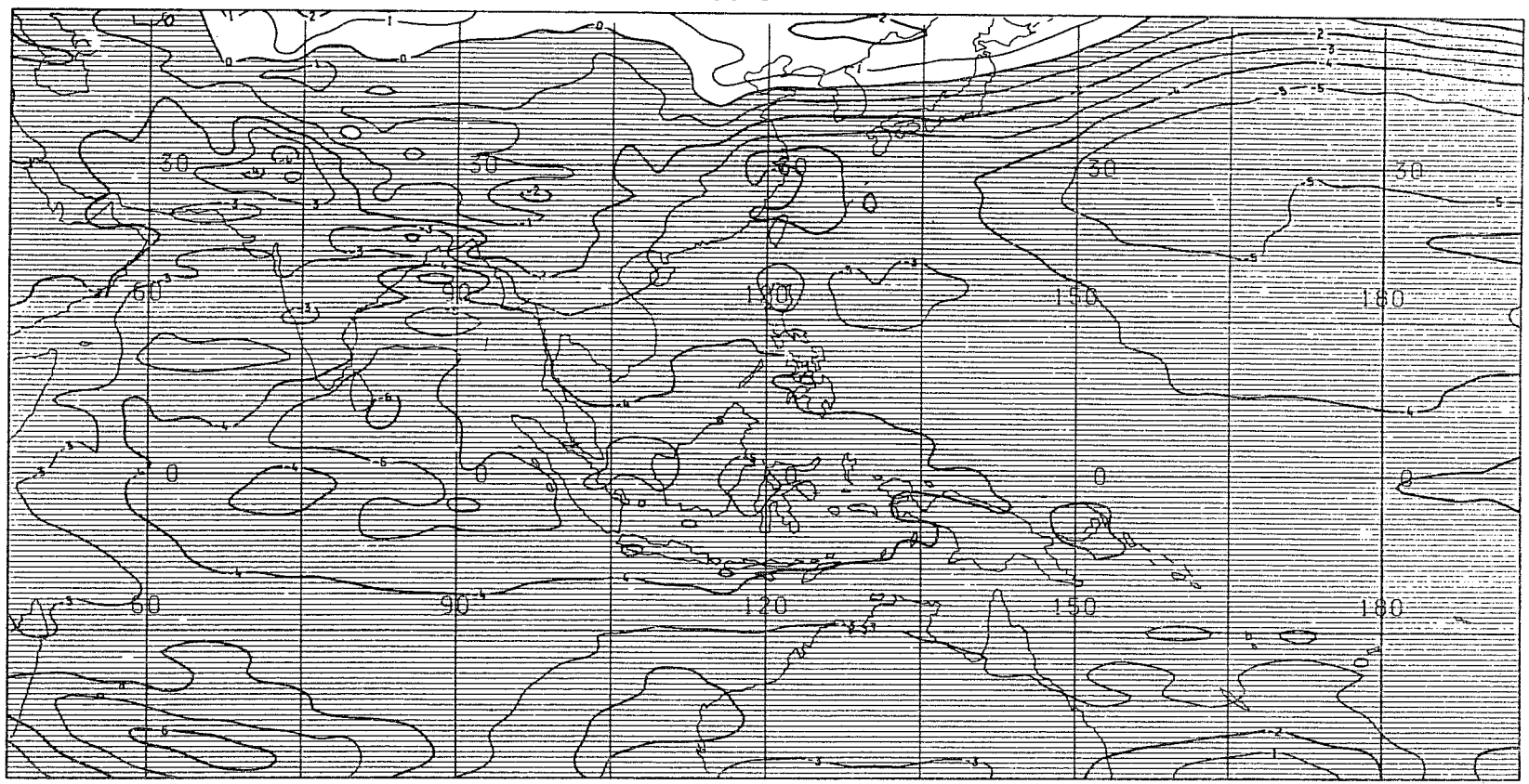

Figure 14 As Figure 12 for σ = 0.317

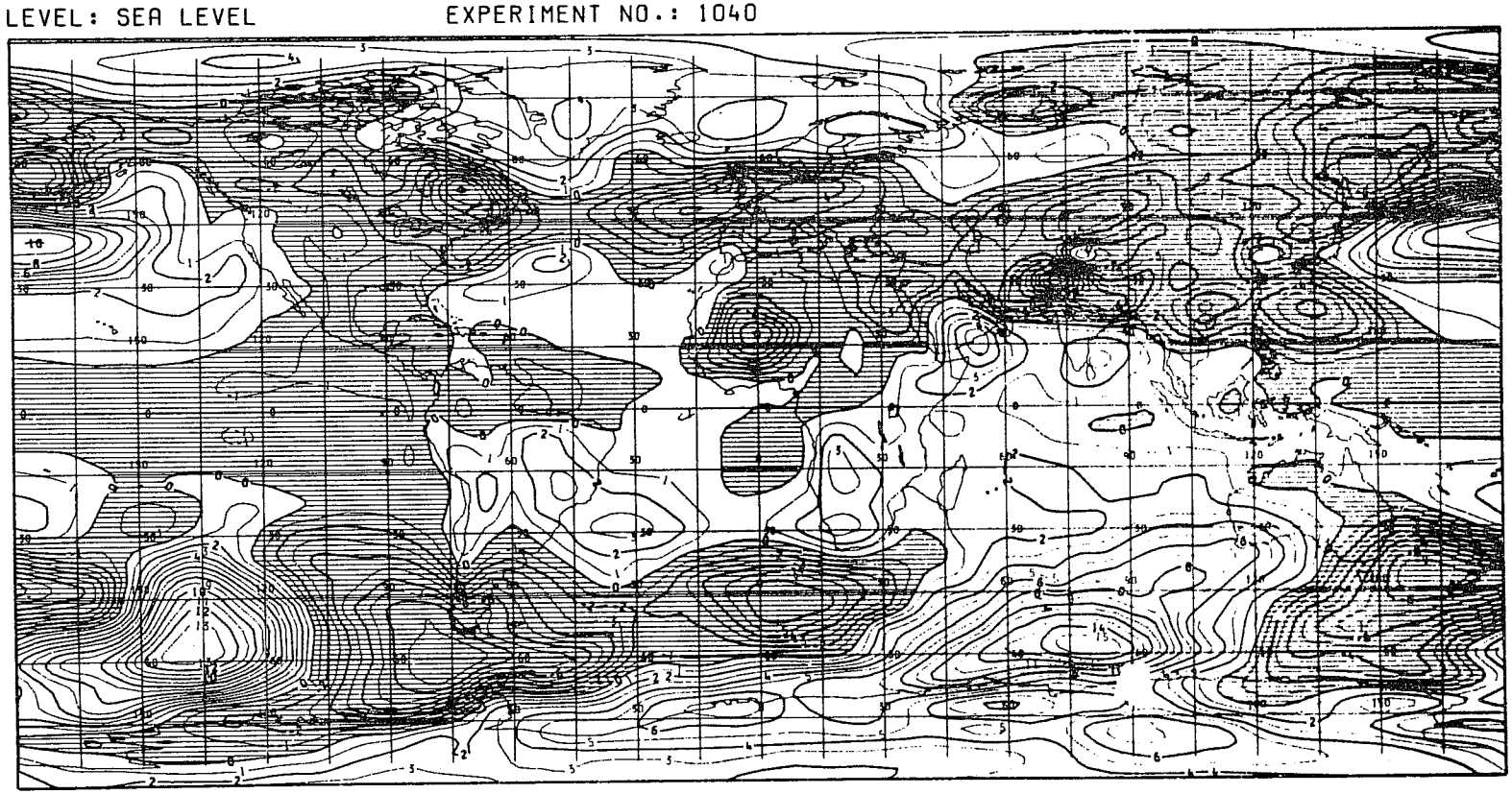

Figure 15 Effect of changing C_{EV} from 9 to 0 on sea level pressure averaged for Days 21 - 50
Contour interval 1 mbar; decreases shaded.

PMSL (MB)
ISOPLETHS EVERY 4
VALID AT 0Z ON 10/6/79 MODEL TIME: DAY 50 HR 0
LEVEL: SEA LEVEL EXPERIMENT NO.: 1040

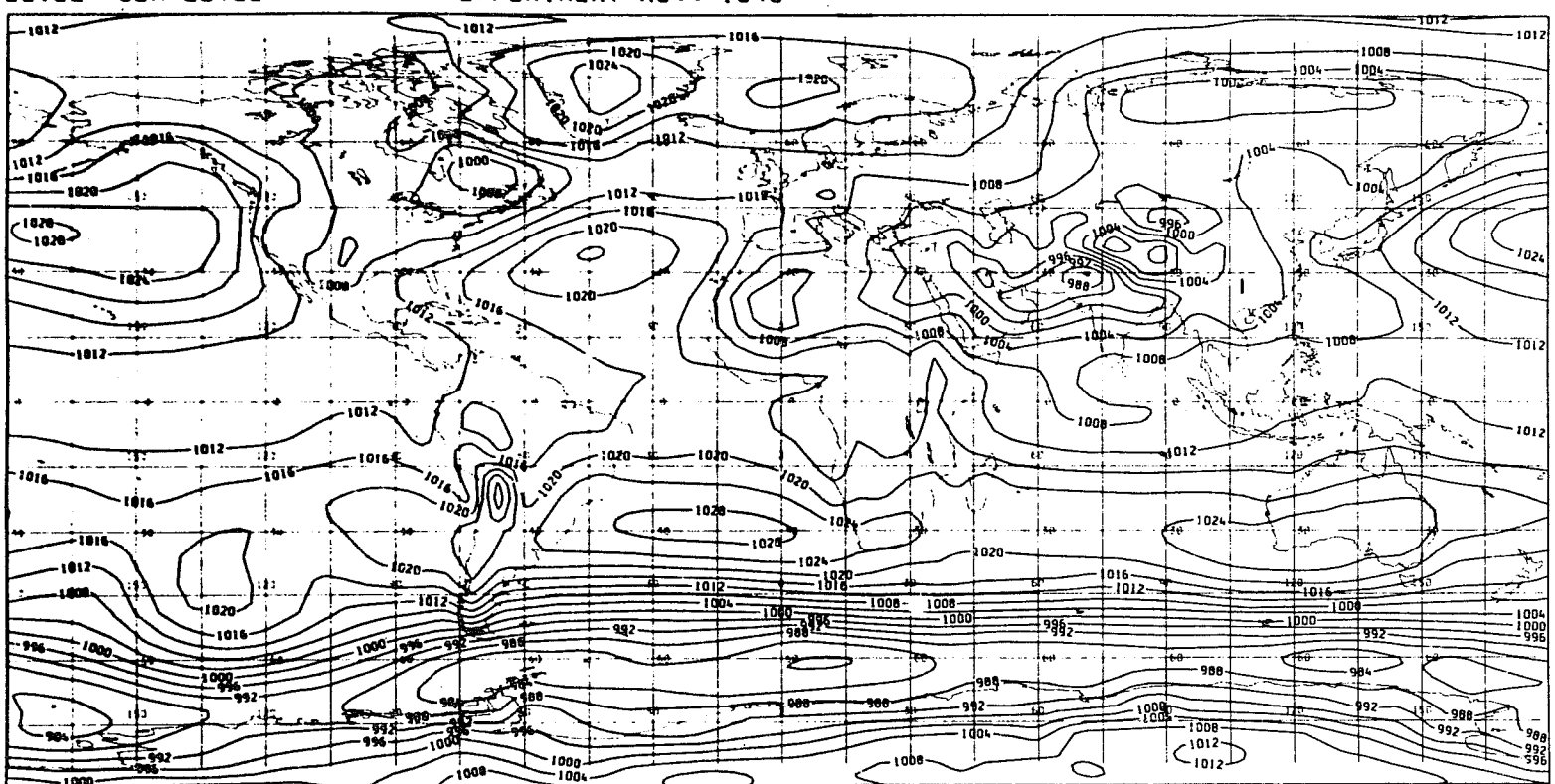

Figure 16(a) Sea level pressure averaged for Days 21 - 50 with $C_{EV} = 0$

PMSL (MB)
ISOPLETHS EVERY 4
VALID AT 0Z ON 10/6/79 MODEL TIME: DAY 50 HR 0
LEVEL: SEA LEVEL EXPERIMENT NO.: 1036

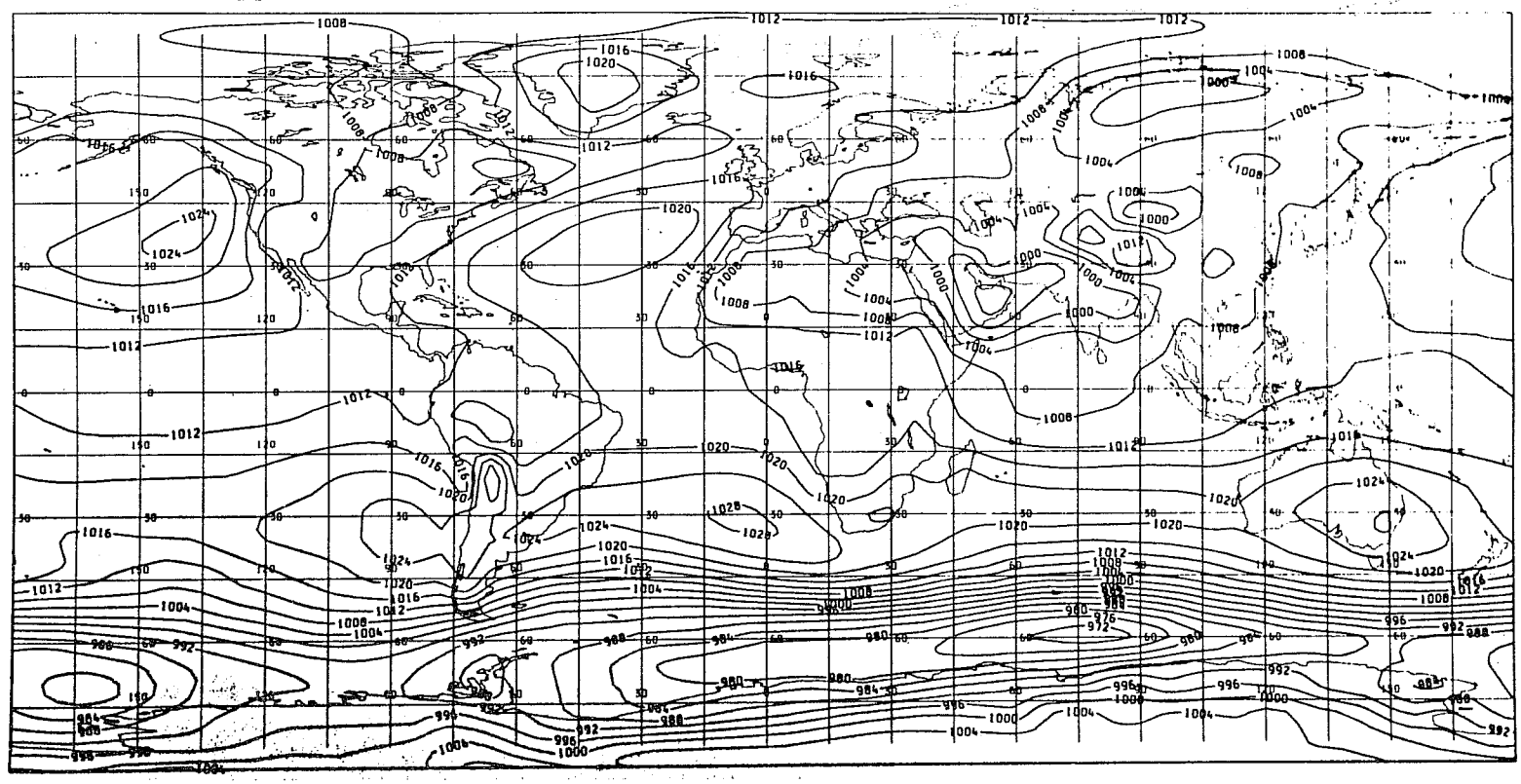

Figure 16(b) As Figure 16(a) with C_{EV} = 9

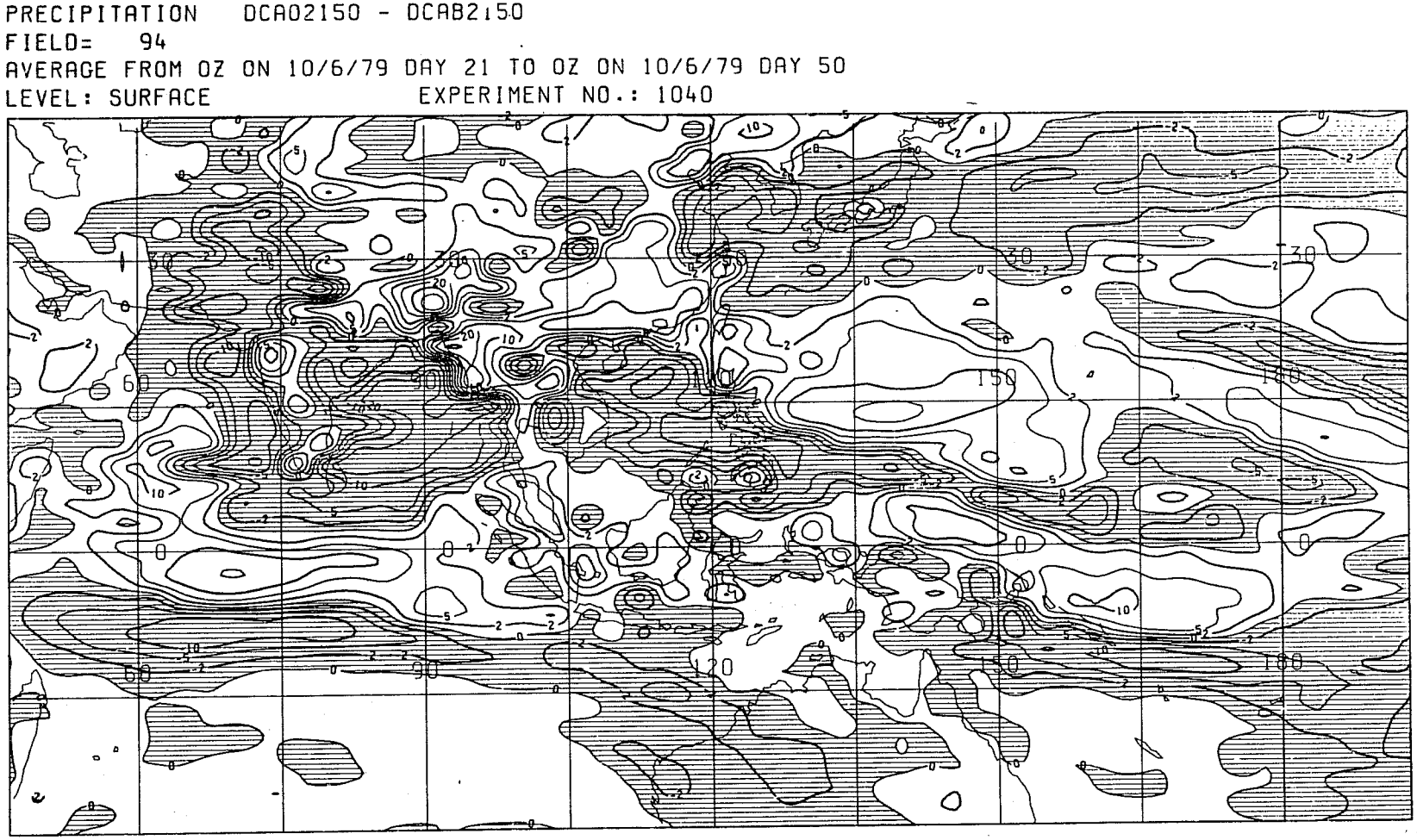

Figure 17 Effect of changing C_{EV} from 9 to 0 on precipitation averaged for Days 21 - 50
Contours at 0, $\pm$ 2,5,10,20,30,40 mm/day; decreases shaded.